

Kinematic synthesis and simulation of a vegetable pot seedling transplanting mechanism with four exact task poses

Liang Sun^{1,2}, Haocong Xu¹, Yuzhu Zhou¹, Jiahao Shen¹,
Gaohong Yu^{1,2*}, Huafeng Hu³, Yuejun Miao⁴

(1. Faculty of Mechanical Engineering & Automation, Zhejiang Sci-Tech University, Hangzhou 310018, China;

2. Zhejiang Province Key Laboratory of Transplanting Equipment and Technology, Hangzhou 310018, China;

3. Hunan Xiangyuan Jinsui Intelligent Equipment Co., Ltd, Loudi 417700, Hunan, China;

4. Hangzhou Anjie Brake Co., Ltd, Hangzhou 310018, China)

Abstract: To obtain a picking and planting integrated transplanting mechanism (PITM) with ideal trajectory shape, reasonable operating attitude, and compact structure for vegetable pot seedling transplanting, a symmetrical structural PITM composed of two planetary carriers and driven by a cam–noncircular gear combination mechanism was proposed in this paper. In accordance with the requirements of transplanting agronomy, the shape of the motion trajectory and the attitude of the end tip of the clamping claw at several specific positions (the starting and end points of picking seedling, the starting point of pushing seedling, and a special point on the return segment) were planned. To make the clamping claws of PITM pass through a set of prescribed positions, the mechanism was simplified to an open-chain 3R mechanism. An accurate four-position-based method for solving the open-chain mechanism model was adopted to obtain the curves of its fixed hinge point (central point) and dynamic hinge point (circle point). The ratio of adjacent bars' lengths was analyzed to determine the feasible interval of the central and circle point curves and the reasonable link length. A desired closed transplanting trajectory that goes through the given points and the corresponding transmission ratio model of the open-chain mechanism was established. After the transmission ratio of each stage of gear and cam pairs was calculated and distributed, the prototype of PITM was designed and manufactured. Lastly, the effectiveness and feasibility of the design were verified through a preliminary experiment of the prototype.

Keywords: kinematic synthesis, transmission ratio, non-circular gear, planetary carrier

DOI: [10.25165/ijabe.20231602.6739](https://doi.org/10.25165/ijabe.20231602.6739)

Citation: Sun L, Xu H C, Zhou Y Z, Shen J H, Yu G H, Hu H F, et al. Kinematic synthesis and simulation of a vegetable pot seedling transplanting mechanism with four exact task poses. *Int J Agric & Biol Eng*, 2023; 16(2): 85–95.

1 Introduction

Pot seedling transplanting has several distinguished advantages for dry field growth, such as having a high survival rate, promoting early maturity of crops, improving land utilization, and increasing the multiple-planting index^[1]. Up to date, many vegetable pot seedling transplanters possessing different functions to achieve transplanting have been proposed. They can be classified into two types: semiautomatic transplanter and fully automatic transplanter, which entirely depends on the automation level of the machines. Manually feeding seedlings is the primary property of the former type, and the low working efficiency and high labor intensity make

it unsuitable for a large-area field. In accordance with the planting device structure, semiautomatic transplanters can further be divided into flexible disc, chain clip, seedling guide tube, and hanging cup types^[2,3].

In contrast with semiautomatic machines, fully automatic ones have higher transplanting efficiency but have more complicated transmission and structure. They adopt multiple sets of mechanisms to complete a series of actions, such as picking, transporting, and planting seedlings^[4-6]. Therefore, additional effort should be devoted to the translation accuracy of the seedling box and the high cohesion between adjacent mechanisms to guarantee the success and survival rates of transplanting.

Kumar and Raheman^[7] proposed a two-row fully automatic vegetable transplanter towed using a walking-type tractor with a power of 9.75 kW for paper-pot seedling transplanting. It consisted of two sets of feeding conveyor, metering conveyor, seedling drop tube, furrow opener, and soil-covering device, as well as an automatic feeding mechanism, a depth adjustment wheel, and a hitching arrangement. Sun et al.^[8] proposed a two-row cotton pot seedling automatic transplanting machine, whose picking seedling mechanism comprised linkage, planetary gear, and cam mechanisms. Combined with two other devices, seedling supply device and planting mechanism, the machine could achieve complete transplanting actions. Chen et al.^[9-11] proposed a minimally different method, in which two rotary mechanisms with different shapes of trajectories were employed to realize the functions of

Received date: 2021-05-04 **Accepted date:** 2022-10-10

Biographies: Liang Sun, PhD, Associate Professor, research interest: design and optimization of agricultural machinery, Email: liangsun@zstu.edu.cn; Haocong Xu, MS candidate, research interest: design and optimization of agricultural machinery, Email: 1183190930@qq.com; Yuzhu Zhou, PhD candidate, research interest: design and optimization of agricultural machinery, Email: 15857187083@163.com; Jiahao Shen, MS, research interest: design and optimization of agricultural machinery, Email: 1036521169@qq.com; Huafeng Hu, research interest: design and optimization of agricultural machinery, Email: 272062455@qq.com; Yuejun Miao, research interest: design and optimization of agricultural machinery, Email: myf600@sohu.com.

***Corresponding author:** Gaohong Yu, PhD, Professor, research interest: design and optimization of agricultural machinery. Faculty of Mechanical Engineering and Automation, Zhejiang Sci-Tech University, Hangzhou 310018, China. Tel: +86-13093730475, Email: yugh@zstu.edu.cn.

picking and planting seedlings.

The machines mentioned above adopt more than two separate mechanisms to implement the entire transplanting process, which makes the machine structure complex and bulky. Integrating the mechanisms for picking, conveying, and planting actions into a single operating mechanism, i.e., picking and planting integrated transplanting mechanism (PITM), cannot only make the working space of a machine compact but can also eliminate the action defect between adjacent mechanisms to improve efficiency. Meanwhile, an operation sequence of ditching, pushing seedlings, and soil covering can be utilized to avoid the planting problem that seedling clips of PITM insert into the soil directly. Zhou et al.^[12] proposed a single-planetary carrier intermittent mechanism with incomplete noncircular gears, by which a large transmission ratio that is essential for forming a pick-and-plant integrated transplanting trajectory was obtained for transplanting flowerpot seedlings. However, the limitation of mechanism structure made it employ an additional spring-shot mechanism to produce a particular trajectory with two sharp shapes for picking and pushing seedlings.

Similarly, Yin et al.^[13] proposed a mechanism based on noncircular gear with an extensive seedling pick-up device be equipped in this transplant arm to meet the aim of transplanting the flowerpot seedlings from the tray into flowerpot. Zhao et al.^[14] proposed a nonuniform speed mechanism using several noncircular gears and a conjugate cam. The suitable combination of the swing caused by the conjugate cam and the variable speed ratio of the noncircular gears also obtained a transmission ratio with high amplitude for achieving complex trajectory. Nevertheless, the shape of the trajectory implied that it is unsuitable for transplanting seedlings with a relatively fragile stem.

In addition to seeking a feasible type of mechanism for designing a transplanting mechanism, the motion synthesis of the selected mechanism is also essential to obtain finally expected trajectory and attitude. Zhao et al.^[15] designed a planetary gear train by using a prescribed curve of transmission ratio, which could be reassigned into several ratio curves for the pitch curves of noncircular gears. Sun et al.^[16] directly employed a given trajectory to obtain a total gear ratio and then divided it into four gear ratio curves for designing a double-planetary carrier mechanism. Given that the attitudes of the mechanism were not considered during the reverse process, the fitting trajectories corresponding to transmission ratios hardly approached the target requirements.

For the attitude issues in the motion synthesis of mechanisms, Han et al.^[17] proposed a rigid body guidance method of bar mechanism based on solution domain synthesis, and the designed linkage mechanism could accurately achieve the given attitude

conditions. Yang et al.^[18] applied a four-position solution domain synthesis method to the dimensional synthesis of the Watt-I six-bar mechanism. Ge et al.^[19,21] proposed a new algorithm for mechanism synthesis based on kinematic mapping and conducted dimension and type syntheses at the same time, which improved the accuracy of the synthesis of a linkage mechanism. Zhao et al.^[22] proposed a unified method for accurate and approximate kinematic synthesis of spherical four-bar mechanisms based on motion mapping.

However, these studies mainly focused on linkage mechanisms, and few studies have been found on planetary gear trains. Although Sun et al.^[23] used the kinematic mapping method to solve the rice pot seedling transplanting mechanism and combined two trajectories that meet the attitude requirements to obtain reasonable trajectory and attitude, the method was only suitable for a mechanism with a single planetary carrier.

In this study, an exact four-pose-based method that considers the shape of the trajectory and attitude of a mechanism is proposed for designing a PITM with two planetary carriers. A guidance mechanism design method is used to solve a simplified gear train model (i.e., open-chain 3R mechanism). The closed trajectory that exactly goes through the prescribed poses is represented by the motion of the open-chain 3R mechanism, then the total and each stage of transmission ratio of the mechanism, which includes shape and attitude information, can be deduced for calculating the kinematic parameters of the gear train mechanism with two planetary carriers.

2 Picking and planting integrated pattern and its requirements

2.1 Transplanting trajectory planning

The picking and planting integrated pattern is a transplanting method using only one mechanism to pick a seedling from a seedling box and directly planting it into a prepared ditch and then pushing and pressing the soil by using a cover roller for vegetable pot seedling transplanting. The success rate of transplanting mainly depends on the picking and planting action of PITM. Figure 1 shows the planning process of a relative trajectory, i.e., static trajectory, for this mechanism. If a pot seedling tray is laid horizontally, a mechanism with two translations of motion, horizontal and vertical, will be used to implement the transplanting actions as shown in Figure 1a. For continuous picking, the seedling box for the feeding pot tray is usually designed to have an oblique angle and a driving roller to recycle the empty tray from the underside of the seedling box. In consideration of the walking speed of the machine, the absolute transplanting trajectory can be described as a dashed curve in Figure 1b. Thus, the static trajectory

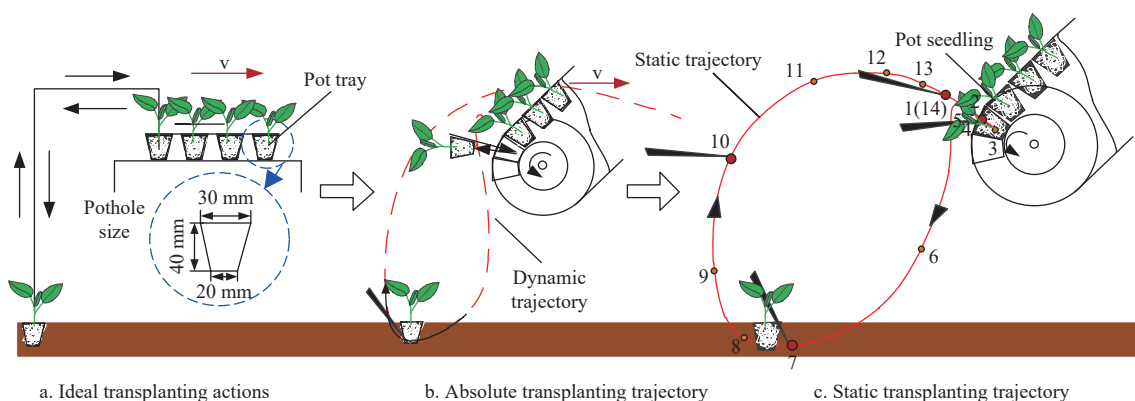


Figure 1 Trajectory plan for vegetable pot seedling transplanting

of PITM can be planned by eliminating the associated motion of PITM's fix element, i.e., a trajectory with a sharp shape for picking seedlings and with a low pushing point for planting seedlings, as shown in Figure 1c. The trajectory has a short approximated straight-line segment, from points 1 to 3, and returns to point 4, which is essential for PITM to have low seedling damage and a high success rate of picking.

The attitude of the picking clip will have a slight change during the picking process to decrease the adhesion force between the soil pot and plastic tray, which can make a seedling easy to be pulled out with a full soil pot. The pulled seedling will be conveyed with the picking clip, and its attitude will be adjusted to be theoretically perpendicular at the pushing position. The seedling will then be pushed into the ditch with the opening of the clips and the pushing of the pushing link. In the preparation for the next transplanting, the returning segment trajectory of the picking clip must avoid interfering with the planted seedlings.

In accordance with the above analysis, the static trajectory can be divided into four segments: picking seedlings, conveying seedlings, pushing seedlings, and returning. As shown in Figure 1c, the segment that includes points 1 to 4 is the picking seedling segment, where points 2 to 3 refer to the grasping process, and points 3 to 4 indicate the pulling process. The segment from points 4 to 8 is the conveying process, where the pushing position is just after point 7 and must be lower than the soil surface. The segment from points 8 to 14 is the returning process for preparing the next cycle. The minimum curvature radius of the segment from points 6 to 10 should be considered for a large planting distance.

2.2 Design requirements for PITM

In accordance with the size of trays (the topside edge, the bottom side edge, and the pothole depth are 30 mm, 20 mm, and 40 mm, respectively), the transplanting agronomic requirements for vegetable pot seedlings, and the kinematic characteristics of the rotary transplanting mechanism, the design requirements for PITM are specified as follows:

- 1) The length of the approximated straight-line segment for grasping seedlings should not be smaller than 45 mm.
- 2) The seedling clip of PITM should not interfere with the plastic pot tray.
- 3) The seedling clip of PITM should be inserted into the soil pot at least 30 mm for grasping seedling steadily.
- 4) The seedling clip's angle at the starting point of the grasping seedling process should be greater than 5° and less than 25°, which makes the seedling clip avoid damaging the leaves of the seedling.
- 5) The seedling clip's angle at the pushing seedling position should be greater than 60°, in which the pushrod can exert a great vertical component force on the soil pot to make the seedling stand upright.
- 6) The seedling clip's angular difference between picking and pushing seedling positions should be greater than 50° and less than 60°. The oblique angle of the seedling box (seedling tray) is approximately 55°. Thus, when the angular difference locates in this angle interval, the pot seedling will be upright at the pushing position.
- 7) The lowest point of the rotary gearbox (planetary carrier) in a rotation cycle should be higher than the soil surface, not less than 40 mm, to prevent the mechanism to interfere with the planted seedlings.
- 8) The trajectory of the picking seedling segment should be nearly perpendicular to the pot tray.

A solution domain synthesis-based method used for studying

the motion synthesis of the open-chain mechanism simplified from PITM will be specifically investigated in the following section.

3 Motion synthesis of the open-chain 3R mechanism

3.1 Relative motion of the open-chain 3R linkage

All rotary transplanting mechanisms have a reverse output characteristic. The output element of the transplanting mechanism continuously rotates in an opposite and variable monotonic or partial swing speed relative to the input element of the transplanting mechanism. The double-planetary carrier transplanting mechanism (Figure 2a) can be simplified as an open-chain 3R mechanism (Figure 2b) without considering the meshing relation of the gear train's transmission in the reverse design of the double-planetary carrier transplanting mechanism^[24].

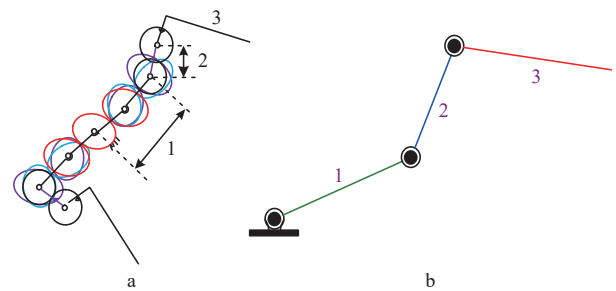


Figure 2 Schematic diagram of gear train mechanism simplified into open chain 3R mechanism

For the single-degree-of-freedom gear train double-planetary carrier transplanting mechanism to achieve reverse output, the following three motion conditions exist between adjacent links in the 3R linkage composed of the first and second planetary carriers (links 1, 2) and a transplanting arm (link 3):

Case 1: While link 1 rotates clockwise (or counterclockwise) all round relative to the ground, link 2 rotates reversely relative to link 1, and link 3 partially swings at a small angle relative to link 2, as shown in Figure 3a.

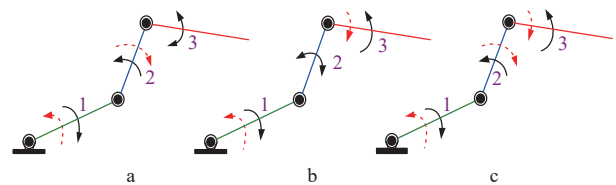


Figure 3 Type of reversing output mechanism

Case 2: While link 1 rotates clockwise (or counterclockwise) all around the ground, link 2 partially swings at a small angle relative to link 1, and link 3 rotates reversely relative to link 2, as shown in Figure 3b.

Case 3: While link 1 rotates clockwise (or counterclockwise) all around the ground, link 2 rotates reversely relative to link 1, and link 3 rotates reversely relative to link 1, as shown in Figure 3c.

The mechanism designed in these motion schemes mentioned above has partially swing, which is not conducive to the action realization of the pushing seedling. The gear drive mechanism designed in Case 3 could not reduce this phenomenon by changing the structure, while the mechanism designed in Case 1 and Case 2 could reduce this phenomenon by adding a cam mechanism. For case 1, the cam mechanism must be set in the link 2 to control the partially swing of the link 3, which means that the second planetary carrier of the transplant will be complex. For Case 2, the cam

mechanism could be set in the first planetary carrier, which is an acceptable structural to reduce this phenomenon. In this paper, Case 2 is selected as the motion scheme of the mechanism to facilitate the design of the cam mechanism of pushing seedlings in the transplanting arm (link 3). Link 1 rotates clockwise, and link 3 rotates counterclockwise relative to link 1. Given the overall motion strategy of the mechanism, the dimensional synthesis of the planar open-chain 3R linkage can be solved by adding link 3 on the basis of the planar open-chain 2R linkage's dimensional synthesis model^[25].

3.2 Motion synthesis method

In Figure 4, A_0 is the fixed hinge point, A_c is the moving hinge point between the first and second links, and Q is the moving hinge point between the second and end links. If the transmission ratio characteristics of adjacent components are not considered, an infinite set of hinge point, A_0 and A_c , position solutions could be obtained for rebuilding a given trajectory with the condition of length and attitude of the end link. Point A_0 is called the central point, and point A_c is called the circle point. For this reason, the curve formed by all points A_0 or A_c is called the central- or circle-point curve, respectively. Let $Q_i(x_i, y_i)$ and θ_i denote the i -th position of point Q and θ_i be the i -th attitude angle of link 2 with respect to the x -axis.

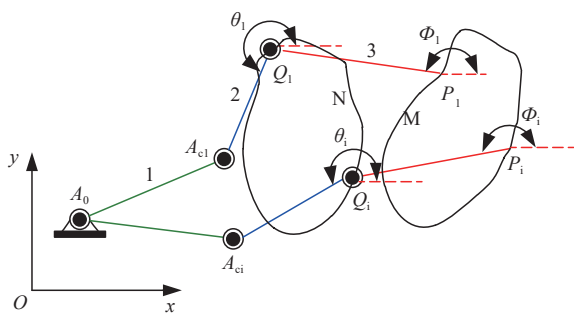


Figure 4 Open-chain 3R mechanism

The displacement matrix of the open-chain 3R mechanism from positions 1 to i ($i=2, 3, 4$) can be obtained in accordance with the general displacement matrix of a rigid body

$$[D_{1i}] = \begin{bmatrix} D_{11i} & D_{12i} & D_{13i} \\ D_{21i} & D_{22i} & D_{23i} \\ D_{31i} & D_{32i} & D_{33i} \end{bmatrix} \tag{1}$$

where, $D_{11i} = \cos \theta_{1i}$, $D_{12i} = -\sin \theta_{1i}$, $D_{13i} = x_i - x_1 \cos \theta_{1i} + y_1 \sin \theta_{1i}$, $D_{21i} = \sin \theta_{1i}$, $D_{22i} = \cos \theta_{1i}$, $D_{23i} = y_i - x_1 \sin \theta_{1i} - y_1 \cos \theta_{1i}$, $D_{31i} = 0$, $D_{32i} = 0$, and $D_{33i} = 1$. $\theta_{1i} = \theta_i - \theta_1$ is the rotational angle of the i -th position of link 2 relative to its first position.

Let the position vectors of central point A_0 (fixed hinge point) and circle-point A_c (moving hinge point) of the first position be $A_0 = [x_0, y_0]^T$ and $A_{c1} = [x_{c1}, y_{c1}]^T$, respectively; the circle-point vector of the i -th position is $A_{ci} = [x_{ci}, y_{ci}]^T$.

$$\begin{bmatrix} A_{ci} \\ 1 \end{bmatrix} = [D_{1i}] \begin{bmatrix} A_{c1} \\ 1 \end{bmatrix} \tag{2}$$

In accordance with the bar length invariant condition, the following constraint equation holds:

$$[A_{ci} - A_0]^T [A_{ci} - A_0] = [A_{c1} - A_0]^T [A_{c1} - A_0] \tag{3}$$

Substituting Equation (2) into Equation (3) and rearranging the terms, we obtain

$$A_{11}(x_0 x_{c1} + y_0 y_{c1}) + A_{12}(y_0 x_{c1} - x_0 y_{c1}) + A_{13} x_0 + A_{14} y_0 + A_{15} x_{c1} + A_{16} y_{c1} + A_{17} = 0 \tag{4}$$

where, $A_{11} = 1 - D_{11i}$, $A_{12} = D_{12i}$, $A_{13} = -D_{13i}$, $A_{14} = -D_{23i}$, $A_{15} = D_{11i} D_{13i} + D_{21i} D_{23i}$, $A_{16} = D_{12i} D_{13i} + D_{22i} D_{23i}$, and $A_{17} = \frac{D_{13i}^2 + D_{23i}^2}{2}$.

For the motion synthesis of the planar mechanism, the central and circle points exist everywhere for a three-position problem ($i=2,3$)^[26], which means that any non-fixed point in the plane can be used as a moving hinge point, and any fixed point in the same plane can be used as a fixed hinge point. The curves formed by the central and circle points are called the Burmester curves, which can be deduced using the displacement matrix method in the case of finite separation.

For a finite separation four-position problem, Equation (4) can be written as

$$C_i x_0 + E_i y_0 + F_i = 0, \quad i = 2, 3, 4 \tag{5}$$

where, $C_i = A_{11} x_{c1} - A_{12} y_{c1} + A_{13}$, $E_i = A_{12} x_{c1} + A_{11} y_{c1} + A_{14}$, and $F_i = A_{15} x_{c1} + A_{16} y_{c1} + A_{17}$.

If x_0 and y_0 are regard as unknown numbers, from the compatibility principle of linear algebra, the determinant of the coefficients in Equation (5) can be written as

$$\begin{vmatrix} C_2 & E_2 & F_2 \\ C_3 & E_3 & F_3 \\ C_4 & E_4 & F_4 \end{vmatrix} = 0 \tag{6}$$

Substituting C_i , E_i , and F_i into Equation (6) yields

$$\begin{vmatrix} A_{21} x_{c1} - A_{22} y_{c1} + A_{23} & A_{22} x_{c1} + A_{21} y_{c1} + A_{24} & A_{25} x_{c1} + A_{26} y_{c1} + A_{27} \\ A_{31} x_{c1} - A_{32} y_{c1} + A_{33} & A_{32} x_{c1} + A_{31} y_{c1} + A_{34} & A_{35} x_{c1} + A_{36} y_{c1} + A_{37} \\ A_{41} x_{c1} - A_{42} y_{c1} + A_{43} & A_{42} x_{c1} + A_{41} y_{c1} + A_{44} & A_{45} x_{c1} + A_{46} y_{c1} + A_{47} \end{vmatrix} = 0 \tag{7}$$

Equation (7) is expanded, and the coefficients of each unknown term are represented in the form of a third-order determinant as follows:

$$\begin{aligned} & |A_{21} A_{32} A_{45}| (x_{c1}^3 + x_{c1} y_{c1}^2) + |A_{21} A_{32} A_{46}| (y_{c1}^3 + x_{c1}^2 y_{c1}) + \\ & (|A_{21} A_{32} A_{47}| + |A_{21} A_{34} A_{45}| + |A_{23} A_{32} A_{45}|) x_{c1}^2 + \\ & (|A_{21} A_{32} A_{47}| + |A_{24} A_{32} A_{46}| + |A_{23} A_{31} A_{46}|) y_{c1}^2 + \\ & (|A_{21} A_{34} A_{47}| + |A_{23} A_{32} A_{47}| + |A_{23} A_{34} A_{45}|) x_{c1} + \\ & (|A_{24} A_{32} A_{47}| + |A_{23} A_{31} A_{47}| + |A_{23} A_{34} A_{46}|) y_{c1} + \\ & (|A_{21} A_{24} A_{46}| + |A_{24} A_{32} A_{45}| + |A_{23} A_{31} A_{45}| + |A_{23} A_{32} A_{46}|) x_{c1} y_{c1} + \\ & |A_{23} A_{34} A_{47}| = 0 \end{aligned} \tag{8}$$

For the simplification of the expression, the elements on the diagonal of the determinant are employed to represent the entire determinant in Equation (8); e.g., the following determinant can be represented by $|A_{21} A_{32} A_{45}|$.

$$\begin{vmatrix} A_{21} & A_{22} & A_{25} \\ A_{31} & A_{32} & A_{35} \\ A_{41} & A_{42} & A_{45} \end{vmatrix}$$

Suppose $H_1 = |A_{21} A_{32} A_{45}|$, $H_2 = |A_{21} A_{32} A_{46}|$, $H_3 = |A_{21} A_{32} A_{47}| + |A_{21} A_{34} A_{45}| + |A_{23} A_{32} A_{45}|$, $H_4 = |A_{21} A_{32} A_{47}| + |A_{24} A_{32} A_{46}| + |A_{23} A_{31} A_{46}|$, $H_5 = |A_{21} A_{24} A_{46}| + |A_{24} A_{32} A_{45}| + |A_{23} A_{31} A_{45}| + |A_{23} A_{32} A_{46}|$, $H_6 = |A_{21} A_{34} A_{47}| + |A_{23} A_{32} A_{47}| + |A_{23} A_{34} A_{45}|$, $H_7 = |A_{24} A_{32} A_{47}| + |A_{23} A_{31} A_{47}| + |A_{23} A_{34} A_{46}|$, $H_8 = |A_{23} A_{34} A_{47}|$, then Equation (8) can be written as

$$H_1 x_{c1}^3 + H_2 y_{c1}^3 + H_1 x_{c1} y_{c1}^2 + H_2 x_{c1}^2 y_{c1} + H_3 x_{c1}^2 + H_4 y_{c1}^2 + H_5 x_{c1} y_{c1} + H_6 x_{c1} + H_7 y_{c1} + H_8 = 0 \tag{9}$$

Equation (9) is the cubic equation of x_{c1} and y_{c1} , called as the equation of the circle-point curve. Any point on the curve can be used as a moving hinge point, and the corresponding fixed hinge points can be solved as follows.

The values of x_{c1} and y_{c1} are substituted into Equation (5) to obtain the following equation:

$$\begin{cases} (C_2 - C_3)x_0 + (E_2 - E_3)y_0 + (F_2 - F_3) = 0 \\ C_4x_0 + E_4y_0 + F_4 = 0 \end{cases} \quad (10)$$

Equation (10) is solved, and the coordinate expression of the central point can be obtained as

$$\begin{cases} x_0 = \frac{F_4(E_2 - E_3) - E_4(F_2 - F_3)}{E_4(C_2 - C_3) - C_4(E_2 - E_3)} \\ y_0 = \frac{F_4(C_2 - C_3) - C_4(F_2 - F_3)}{C_4(E_2 - E_3) - E_4(C_2 - C_3)} \end{cases} \quad (11)$$

In consideration of the cubic equation of the circle-point curve, a value of x_{c1} may correspond to one or two or three values of y_{c1} . In addition, each set of (x_{c1}, y_{c1}) will correspond to a set of (x_0, y_0) to form an open-chain 2R mechanism.

In accordance with the method mentioned above and the agronomic requirements for vegetable seedling transplanting, the length of the transplanting arm (link 3) is selected as 125 mm (a suitable dimension for designing a pushing seedling mechanism), and the four attitude angles of the end point of link 3 are preset as 171°, 130°, 154°, and 167°. The position and orientation information of link 2 is listed in Table 1.

Table 1 Four groups of position and orientation data for link 2

No.	x_i	y_i	$\theta_i/(\circ)$
1	124.03	86.22	230
2	-33.07	-96.40	120
3	-125.45	39.02	14
4	97.03	116.80	241

3.3 Determining the lengths of two planetary carriers

In accordance with the rotation strategy of the transplanting mechanism and the preset key poses, the horizontal coordinates of the fixed and moving hinge points are constrained in the range [-60, 25] and [30, 80], respectively. Their vertical coordinates are constrained in the range [-100, 100], as shown in Figure 5.

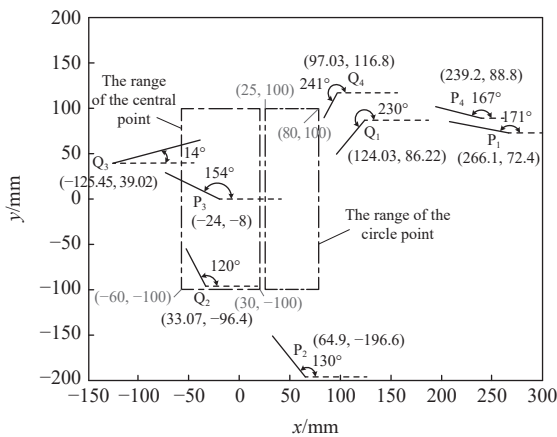


Figure 5 Position constraint space of the hinge point

The circle-point curve can be obtained by substituting the parameters listed in Table 1 into Equation (9). A series of discrete circle-point coordinates (x_{c1}, y_{c1}) is determined by continuously evaluating the step size $\Delta x_{c1}=0.01$ in the range [-60, 25] mm, and the central-point coordinates corresponding to the series of circle-point coordinates are determined using Equations (10) and (11). From the circle- and central-point curves shown in Figure 6, a single value can determine three circle points when the horizontal coordinate is in the range [-34, 72]. Only one circle point can be obtained when the horizontal coordinate is less than -34 or greater

than 72. The distance between the circle point and the corresponding central point is equal to the length of the side link. The figure illustrates that countless circle and central points can make the open-chain 2R mechanism pass through the four given poses, but not every set of data can meet the requirements of the pot seedling transplanting mechanism due to the limitation of the mechanism size and workspace. On the basis of the size requirements of the transplanting mechanism, i.e., the lengths of links 1 and 2 are limited in the range [70, 100] mm, the reasonable intervals of the circle and central points corresponding to the two links are determined as [-65, 25] and [-100, 100] respectively, which are depicted in thick line in Figure 6.

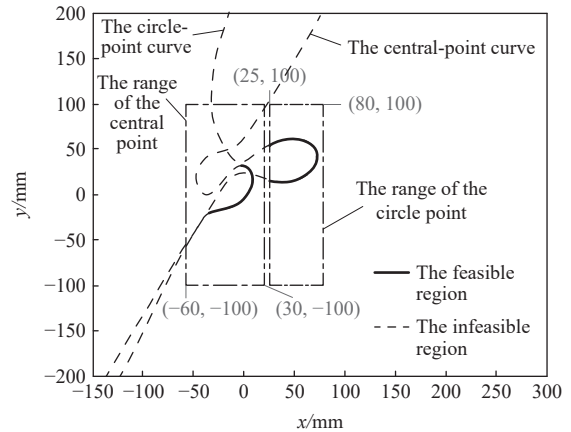
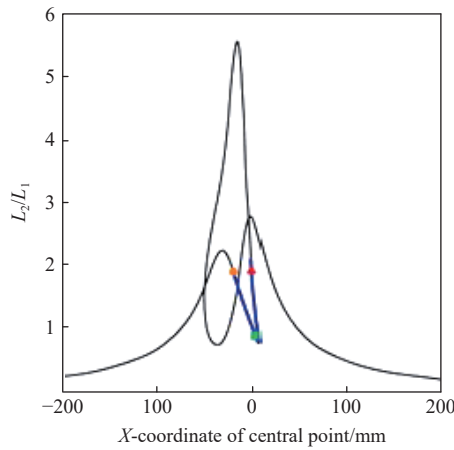


Figure 6 Feasible region of the circle and central curves

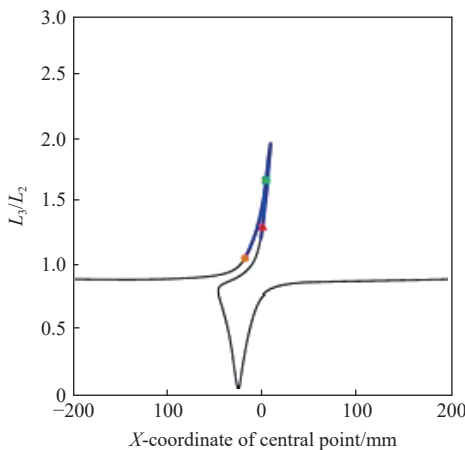
When the link length ratio $k_1=L_2/L_1$ of links 2 and 1 in the open-loop 3R mechanism and the link length ratio $k_2=L_3/L_2$ of links 3 and 2 have small values, the mutual interference between the two planting arms in the transplanting mechanism can be avoided easily. Meanwhile, the compactness of the overall structure of the mechanism can be improved. Therefore, when selecting the appropriate coordinates of central and circle points in the feasible region shown in Figure 6, the proportional relationship of link length under different position point pairs (one central point corresponds to one circle point) should be analyzed. In Figure 7, the thick solid line segments from the small circle to the triangle alter the length ratio of links 2 to 1 and links 3 to 2 when the central points are located in the feasible region. When the ratio of links 2 and 1 is smallest, the ratio of links 3 to 2 is largest.

For example, if the central and circle points are set at (0.01801, 31.6135) and (34, 59.42), respectively, an open-chain mechanism ①, as shown in Figure 8, can be determined. The ratio of links 2 to 1 is 2.1392, and the ratio of links 3 to 2 is 1.3307. The central point (-19.5744, -14.7805) and the circle point (30, 14.7183) are composed of mechanism ② in Figure 8. The ratio of links 2 to 1 is 2.0447, and the ratio of links 3 to 2 is 1.0582. However, the length of link 1 in both mechanisms is extremely small, whereas the length of link 2 is excessively long. This condition easily causes a planting arm interference when designing a transplanting mechanism.

In consideration of the link length ratio of links 2 to 1 and links 3 to 2, the overall size of the transplanting mechanism, and the agronomic requirements of transplanting, a suitable set of central points (3.9926, 0.4983) and circle points (70, 33.4092) is selected to form an open-loop 3R mechanism. The mechanism parameters are as follows: $L_1=73.6237$ mm, $L_2=75$ mm, and $L_3=125$ mm. The corresponding open-loop 3R mechanism ③ is also shown in Figure 8.



a. Length ratio of links 2 to 1



b. Length ratio of links 3 to 2

Figure 7 Length ratio of the open-loop mechanism

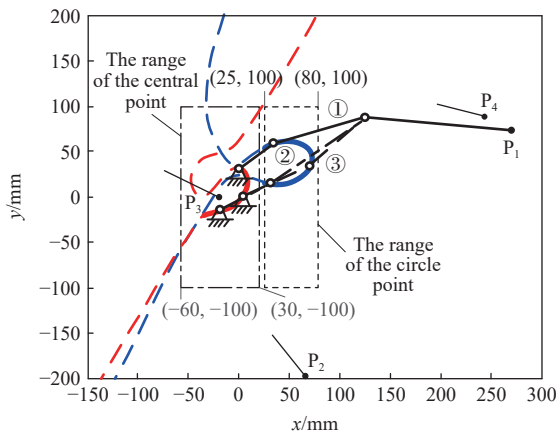


Figure 8 Synthesis of the open-loop 3R mechanism

4 Design of a transplanting mechanism

4.1 Trajectory fitting and transmission ratio calculation

Combined with the transmission characteristics of the gear train and the structural characteristics of the open-loop 3R mechanism, the first planetary carrier L_1 rotates at a constant speed in the range $[0, 2\pi]$, the second planetary carrier L_2 swings within a certain angle relative to the first planetary carrier, and the planting arm L_3 rotates at a reverse speed relative to the first planetary carrier. Suppose the angular displacement of the first planetary carrier is α_1 , the angular displacement of the second planetary carrier relative to the first planetary carrier is α_2 , and the angular displacement of the planting

arm relative to the second planetary carrier is α_3 . The total transmission ratio of input and output links is as follows:

$$i = \frac{\omega_1}{\omega_3} = \frac{d\alpha_1}{d(\alpha_1 + \alpha_2 + \alpha_3)}$$

where, i is the total transmission ratio; ω_3 is the absolute angular velocity of link L_3 , rad/s; ω_1 is the absolute angular velocity of link L_1 , rad/s.

To obtain a complete and continuous motion, aside from the 4 prescribed vital points, 10 other data points are added to combine a set of data points. For the open-loop 3R mechanism, two relative angular displacement curves are required to be constructed. Link L_2 swings relative to link L_1 , and link L_3 fully rotates relative to link L_2 . Accordingly, the value differences between the starting and end points of the two angular displacement curves are equal to zero and 2π .

For obtaining a close and smooth trajectory, the tangent vector orientation of the two end points of each curve obtained on the basis of the nonuniform B-spline fitting method is preset to be the same. A transplanting trajectory of the open-loop 3R mechanism and the total and each stage of transmission ratio can be obtained by combining the angular displacement curves. Various angular displacement curves, trajectories, and planting attitudes can also be produced by adjusting the value of the 10 added data points. Figure 9 shows a reasonable trajectory, two angular displacement curves, and the total transmission ratio.

4.2 Distribution of transmission ratio

Figure 9 shows a schematic of the transplanting mechanism, in which a cam mechanism is employed to fulfill the swing of the second planetary carrier, and gear trains are used to realize unlimited rotation of the planting arm. In the first planetary carrier 1, two transmission routes (S blue arrow and R red arrow) that start from the central element composed of cam 6 and solar gear 2 and converge at the input of the second planetary carrier (fixed with gear 8) together control the complex motion of the planting arm (fixed with gear 11). Therefore, the main work in this section is to distribute the total transmission ratio obtained in the above section into each stage of transmission.

To facilitate the distribution of transmission ratio, the gears in the second planetary carrier are assigned as the same spur gears. Thus, the determination of the transmission ratio of each gear (or cam) pair in the first planetary carrier becomes the main work. Moreover, we assume an opposite angular velocity on the first planetary carrier to make it stationary, which transfers this part of the planetary gear trains into ordinary gear trains; i.e., all the rotating shafts in the first planetary carrier are mounted on a common stationary frame. Afterward, the transmission ratios of the new gear train can be written as follows:

$$i_{23}^1 = \frac{\omega_2 - \omega_1}{\omega_3 - \omega_1} \tag{12}$$

$$i_{28}^1 = \frac{\omega_2 - \omega_1}{\omega_8 - \omega_1} \tag{13}$$

$$i_{35}^1 = \frac{\omega_3 - \omega_1}{\omega_5 - \omega_1} \tag{14}$$

where, $i_{23}^1, i_{28}^1, i_{35}^1$ are the transmission ratios between components 2 and 3, components 2 and 8, and components 3 and 5, respectively; and $\omega_1, \omega_2, \omega_3, \omega_5,$ and ω_8 are the angular velocities of the corresponding components.

On the basis of stationary planetary carrier 1, the transmission ratio between components 5 and 11 can be obtained by adding a

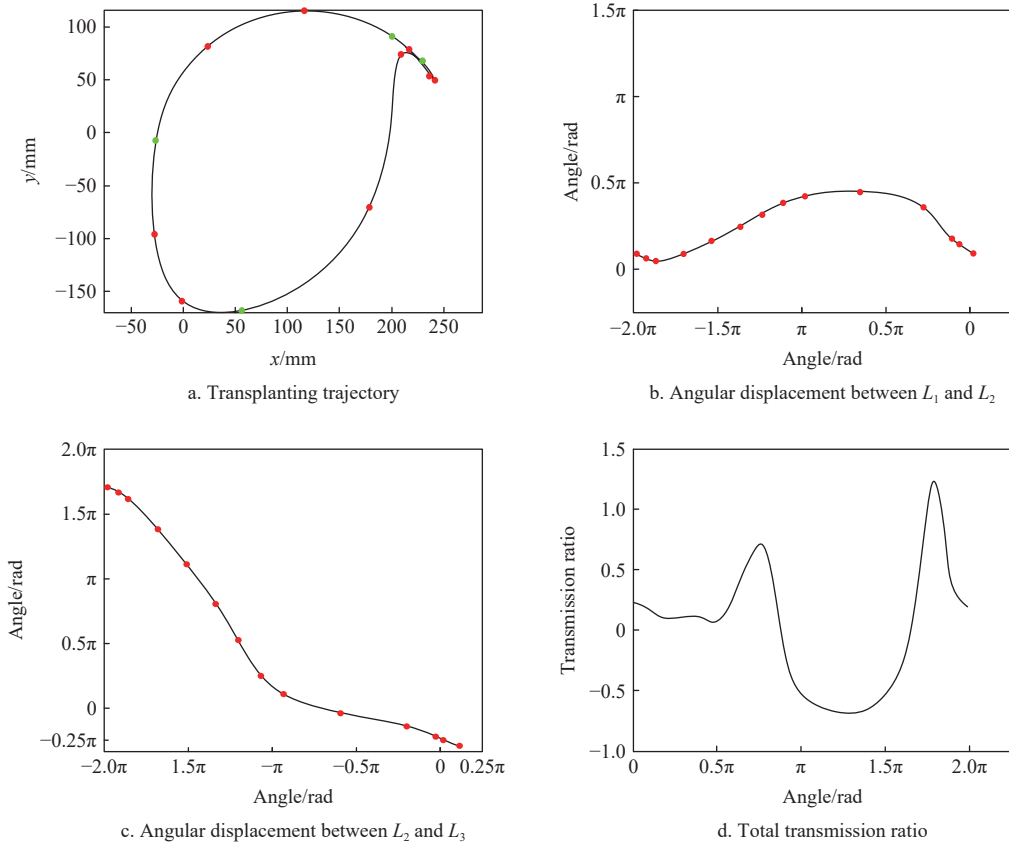
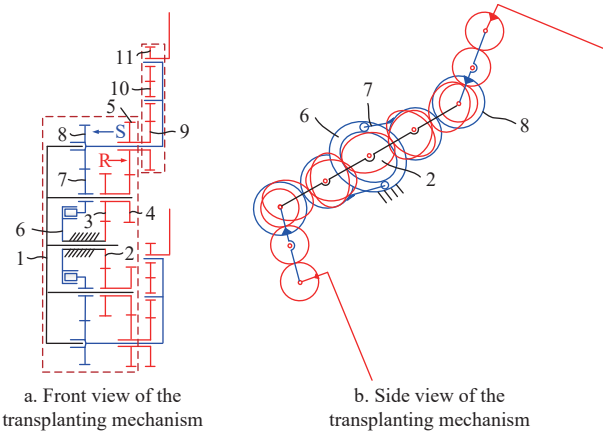


Figure 9 Optimized trajectory and parameter curve



1. First planetary carrier 2, 3, 4, 5, 8, 9, 10, 11. Transmission gears 6. Cam 7. Cam follower with a sector gear

Figure 10 Schematic of the transplanting mechanism

common angular velocity $-\omega_8$ to the second planetary carrier to alter it to the ordinary gear train, i.e.,

$$i_{5,11}^8 = \frac{(\omega_5 - \omega_1) - (\omega_8 - \omega_1)}{(\omega_{11} - \omega_1) - (\omega_8 - \omega_1)} = \frac{\omega_5 - \omega_8}{\omega_{11} - \omega_8} \quad (15)$$

where, ω_{11} is the angular velocity of component 11. The rotational speed ratio of input component 1 and output component 11 can be associated by solving Equation (14) - (17).

$$\omega_{11} = \frac{\omega_2 - \omega_1}{i_{23}^1 \cdot i_{35}^1 \cdot i_{5,11}^8} - \frac{\omega_2 - \omega_1}{i_{28}^1 \cdot i_{5,11}^8} + \frac{\omega_2 - \omega_1}{i_{28}^1} + \omega_1 \quad (16)$$

Given that component 2 is a solar gear fixed on the rack, ω_2 is equal to zero. Substituting the value of ω_2 into Equation (18) and rearranging it, we can obtain

$$\frac{\omega_{11}}{\omega_1} = \frac{1}{i_{28}^1 \cdot i_{5,11}^8} - \frac{1}{i_{35}^1 \cdot i_{23}^1 \cdot i_{5,11}^8} - \frac{1}{i_{28}^1} + 1 \quad (17)$$

where, i_{28}^1 is the transmission ratio of the cam mechanism and sector gear pair, which can be obtained from the angular displacement curve, as shown in Figure 9b.

For simplifying the assigning process of the transmission ratio, gears 9, 10, and 11 are designed as spur gears with the same parameters, i.e., $i_{5,11}^8$ is equal to 1.

The value of $i_{5,11}^8$ is substituted into Equation (19), and the two-stage transmission ratio I of the first planetary carrier can be written as

$$I = i_{35}^1 \cdot i_{23}^1 = \frac{\omega_1}{\omega_1 - \omega_{11}} \quad (18)$$

Figure 11 shows the two-stage transmission ratio I obtained in terms of the above-mentioned assigning method.

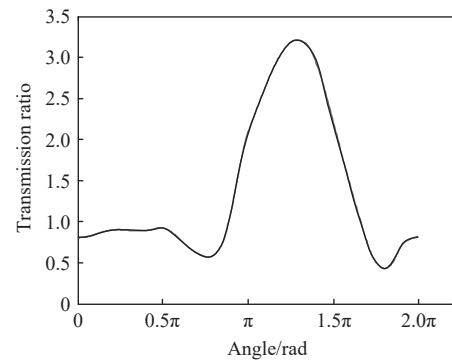


Figure 11 Transmission ratio curve of the planetary gear train

4.3 Convexity of noncircular gears

Noncircular gear pitch curves can be directly obtained in accordance with transmission ratio. However, the convexity of a

noncircular gear pitch curve that affects the transmission and manufacture should be considered in the design processing. A noncircular gear pitch curve that meets the convexity requirement should be selected to design the transplanting mechanism. In this paper, a convexity index is constructed on the basis of the definition of curvature radius, which is the function of the transmission ratio.

The curvature radii of the driving and driven noncircular gears are respectively expressed as follows:

$$\rho_1 = \frac{a \left[1 + \left(\frac{I_1}{1+I_1} \right)^2 \right]^{\frac{3}{2}}}{1 + I_1 + I_1'} \quad (19)$$

$$\rho_2 = \frac{a I_1 \left[1 + \left(\frac{I_1'}{1+I_1} \right)^2 \right]^{\frac{3}{2}}}{1 + I_1 - I_1 I_1' + (I_1')^2} \quad (20)$$

where, a is the center distance of the meshing noncircular gear pairs, and I_1 is the transmission ratio of the meshing noncircular gears.

If the values of ρ_1 and ρ_2 are not smaller than zero, the pitch curves of the noncircular gears must be completely convex. Thus, the convexity indexes for evaluating the driving and driven noncircular gears can be respectively written as

$$p_a = 1 + I_1 + I_1' \geq 0 \quad (21)$$

$$p_b = 1 + I_1 - I_1 I_1' + (I_1')^2 \geq 0 \quad (22)$$

After each stage of transmission ratio is substituted into Equation (23) and Equation (24), the convexity index of the noncircular gear pairs can be obtained as

$$p = \min\{p_a, p_b\} \quad (23)$$

Figure 12 shows the pitch curves of noncircular gears 2, 3, 4, and 5 calculated in terms of the transmission ratio shown in Figure 9 under the convexity index. The smoothness of the pitch curve is optimized using the method proposed in our previous study.

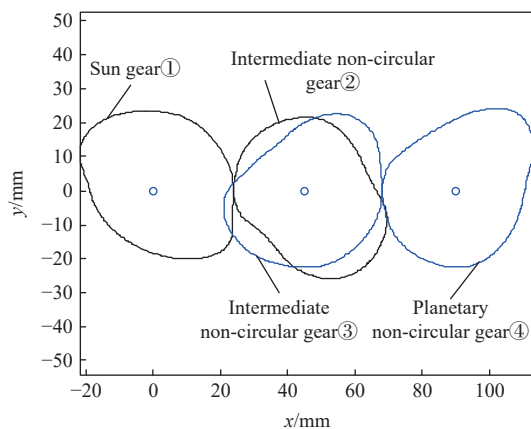


Figure 12 Noncircular gear pitch curve with $p=1.724$

4.4 Generation of cam profile

To facilitate the calculation of the swing cam mechanism, the transmission ratios of sector gears 7 and 8 are assigned as constant 1, such that the transmission ratio of the cam mechanism is equal to i_{28}^1 . In accordance with the cam design equation, the profile of the cam and corresponding parameters can be obtained. Figure 13 shows the profile of the cam with max pressure angle $\alpha_{max}=43^\circ$, and the data points corresponding to the interpolation points of the transmission ratio are listed in Table 2.

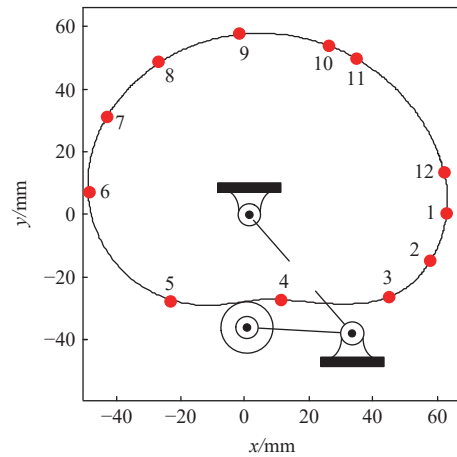


Figure 13 Cam mechanism with $\alpha_{max}=43^\circ$

Table 2 Coordinates of the cam profile

No.	x	y	No.	x	y
1	61.588	0	7	-44.378	30.769
2	55.499	-16.855	8	-28.336	47.877
3	45.707	-25.757	9	-1.0358	57.475
4	11.14	-27.633	10	30.759	50.967
5	-30.946	-24.83	11	55.46	26.83
6	-50.31	8.6878	12	60.849	12.876

5 Simulation and test of the transplanting mechanism

5.1 Simulation analysis

To simulate the transplanting mechanism, in addition to the constraints imposed on the gear pairs and cam mechanism associated with the planetary carriers, the spring-cam mechanism designed in the planting arm for achieving picking and pushing seedling is also essential to be considered. In this study, the simulation model is built using the ADAMS software. Impact forces with default parameters are employed to associate with the gear and cam pairs. Let the stiffness of the pushing seedling spring be 2 N/mm and the free length be 70 mm. Given that the length of the spring at the finish picking seedling position is 25 mm, the preload of the spring at length 25 mm is set to 100 N. The average rotational speed of the transplanting mechanism is 60 r/min, i.e., 120 plants per minute per row. Thus, the motion of the first planetary carrier is set to 360 °/s, and the simulation time is 1 s and 400 steps.

Figure 14 shows the static transplanting trajectory of the mechanism. The shape of the trajectory is completely identical to that of the prescribed one shown in Figure 8a, which verifies the correctness of the assignment of the transmission ratio. The minimal fluctuation in the trajectory at the position of the pushing seedling is mainly caused by the impact force that the pushrod acts on the planting arm. The force and deformation of the spring in the entire pushing seedling stroke are shown in Figure 15.

Two curves of the attitude angle of the planting arm in a circle obtained through theoretical calculation and simulation are shown in Figure 16. The variation trend of the two curves is identical, but it has a numerical deviation caused by the angle difference (20°) between the actual design structure of the transplanting arm and the theoretical value, as well as the tooth profile clearance in the simulation process.

5.2 Transplanting experiment

To verify the correctness of the theoretical results and detect the transplanting efficiency of the transplanting mechanism, a physical prototype is processed, and the manipulator is installed on

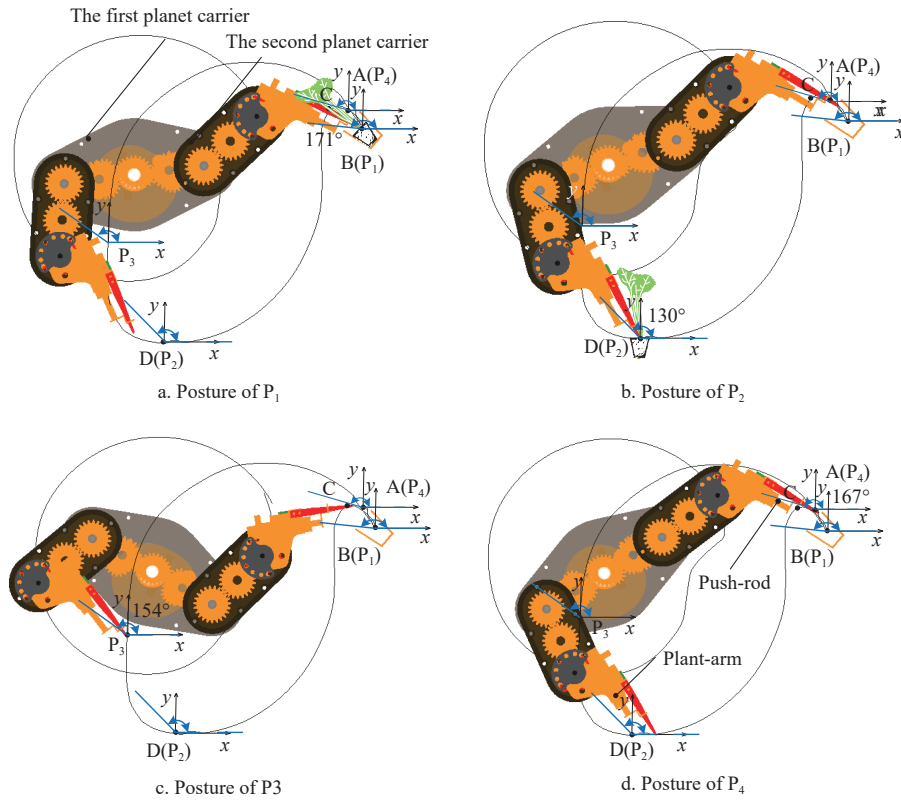
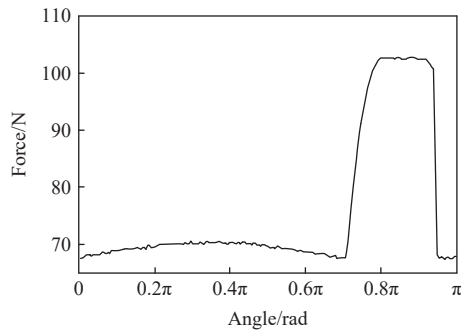
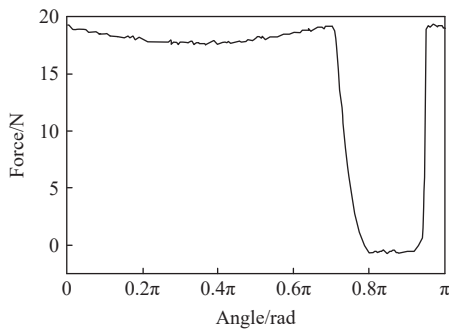


Figure 14 Simulation trajectory of the transplanting mechanism



a. Force



b. Deformation

Figure 15 Force and deformation of the spring in the entire seedling stroke

the test bench, as shown in Figure 17. The seedling extraction and planting tests are performed. The idling trajectory is obtained by high-speed camera shooting, which is compared with the theoretical trajectory. The shape is consistent, as shown in Figure 18.

When the seedling extraction efficiency of the transplanting mechanism is tested, broccoli pot seedlings with seedling ages of 30 d and 40 d, seedling heights of 100 and 200 mm, and soil water

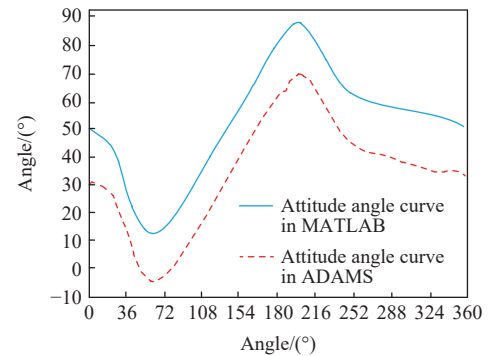


Figure 16 Attitude angle curve



Figure 17 Prototype of PITM Figure 18 Trajectory comparison

content of 50% are selected and tested at different rotational speeds. The rotational speed of the transplanting mechanism is set to 30 r/min, 45 r/min, and 60 r/min, and the seedlings are taken 175 times at each rotational speed. A total of 166, 162, and 154 plants are successfully taken out. That is, the success rates of taking seedlings are 94.8%, 92.6%, and 88.0%. The test results indicate that when the speed reaches 60 r/min, the success rate of transplanting

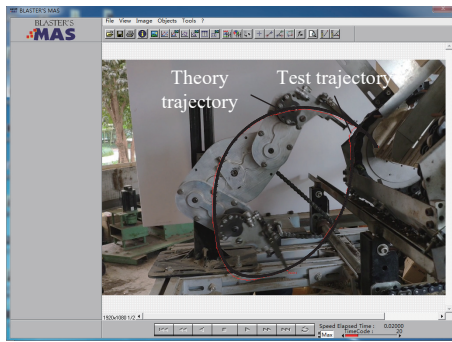


Figure 18 Trajectory comparison

decreases evidently, which is mainly caused by the aggravation of the vibration of the mechanism. Figure 19 shows the three critical actions of the transplanting process: grasping, conveying, and pushing seedling.



a. Grasping seedling



b. Conveying seedling



c. Pushing seedling

Figure 19 Picking seedling test



Figure 20 Planting seedling test

1) The clearance of the moving high pair is sensitive to the influence of the mechanism's output trajectory because the transplanting mechanism adopts the noncircular gear–cam combination transmission mechanism. Therefore, high requirements are put forward for the processing and assembling of each part of the mechanism. In the subsequent application, the influence of machining error on the trajectory could be weakened or eliminated by designing a backlash control device.

2) The error among the initial position, the initial angle, and the theoretical value during the installation of the mechanism directly affects the success rate of the seedling picking and transplanting in this kind of soil bowl type; i.e., the position of the mechanism relative to the seedling box requires reasonably high installation accuracy. The trajectory length of the seedling picking should be sufficient to avoid breaking the soil pot with the seedling box after taking the seedlings and altering the angle of the held seedlings, which may affect the erectness of planting.

3) After planting seedlings, the soil should be covered in time, not extremely early or late; otherwise, the seedling standing degree in the soil will be affected.

6 Conclusions

1) In accordance with the requirement of vegetable pot seedling

An indoor preliminary planting experiment is conducted to verify the planting effect. A self-made circular rotating soil tank is used as a dry field. The transplanting mechanism rotates with a fixed axis relative to the frame, and the seedling box moves laterally and longitudinally intermittently. Combined with the rotary movement of the soil trough, the planting test can be implemented in the laboratory. The planting experiment is performed by ditching, throwing seedlings, and covering with soil. Given that the soil tank cannot rotate excessively fast, the linear speed of the soil tank is set to 150 mm/s. The rotational speed of the transplanting mechanism is 15 r/min; i.e., the seedlings are planted every 2 s. The soil tank moves 300 mm (i.e., the plant space of the seedlings is 300 mm). Fifteen plants are planted in each group, and the seedling standing rate almost reaches 93%. The planting effect is shown in Figure 20.

On the basis of many experiments and their analysis, the mechanism to complete the picking–planting integrated transplanting should pay attention to the following problems:

transplanting, a kind of PITM with double-planetary carriers driven by a combination mechanism composed of cam and noncircular gear trains was proposed. The characteristic of the variable-speed swing produced by the combination mechanism was adopted to design a trajectory with a sharp beak, which is essential for picking pot seedlings from a pot tray.

2) The kinematic synthesis of the open-chain 3R mechanism was conducted using the solution domain synthesis theory of linkage mechanism, and the kinematic relations of each component under the given trajectory constraints were determined. The synthesis of PITM was achieved by attaching the transmission gear and cam mechanism to the open-chain mechanism.

3) A physical prototype of PITM was developed, and the consistency between the measured and theoretical trajectories verified the correctness of the design method of the transplanting mechanism. Meanwhile, the feasibility of PITM was preliminarily verified from the success rate of picking seedlings and the effect of planting seedlings through an indoor transplanting experiment.

Acknowledgements

This work was supported by the National Key Research and Development Program of China (Grant No. 2022YFD2001802), the National Natural Science Foundation of China (Grant No. 51975534), the Key Research and Development Plan of Zhejiang Province (Grant No. 2022C02048), the Science and Technology Planning Project of Quzhou City (Grant No. 2021K49), and the Science and Technology Planning Project of Qujiang District (Grant No. QJ2021008).

[References]

- [1] Xiao T Q, He C X, Cui X Y, Chen Y S, Cao G Q, Hu H. Study on mechanization planting process of vegetable. *Agricultural Mechanization Research*, 2016; 38(3): 259–262.

- [2] Khadatkar A, Mathur S M, Gaikwad B B. Automation in transplanting: a smart way of vegetable cultivation. *Curr Sci*, 2018; 115(10): 1884–1892.
- [3] Zhang M, Ji J T, Du W X. Status and prospect of transplanter at home and abroad. *Agricultural Engineering*, 2012; 2(2): 21–23.
- [4] Jin X, Li D Y, Ma H, Ji J T, Zhao K X, Pang J. Development of single row automatic transplanting device for potted vegetable seedlings. *Int J Agric & Biol Eng*, 2018; 11(3): 67–75.
- [5] Jin X, Ji J T, Huang Z Z, Du X W, Du M M. Seedling pick-up mechanism of five-bar combined with ordinary gear train. *International Agricultural Engineering Journal*, 2017; 26(2): 151–158.
- [6] Jin X, Ji J T, Liu W X, He Y K, Du X W. Structural optimization of duckbilled transplanter based on dynamic model of pot seedling movement. *Transactions of the CSAE*, 2018; 34(9): 58–67. (in Chinese)
- [7] Kumar G V P, Raheman H. Development of a walk-behind type hand tractor powered vegetable transplanter for paper pot seedlings. *Biosyst Eng*, 2011; 110(2): 189–197.
- [8] Sun L, Wang Z F, Wu C Y, Zhang G F. Novel approach for planetary gear train dimensional synthesis through kinematic mapping. *Proc Inst Mech Eng, Part C: J Mech Eng Sci.*, 2020; 234(1): 273–288.
- [9] Chen J N, Wang Y, Huang Q Z, Huang H M, Wu C Y, Zhang P. Optimization and test of transplanting mechanism with planetary deformed elliptic gears for potted-seedling transplanter. *Transactions of the CSAM*, 2013; 44(10): 52–56, 92. (in Chinese)
- [10] Chen J N, Huang Q Z, Wang Y, Sun L, Zhao X, Wu C Y. Parametric analysis and inversion of transplanting mechanism with planetary non-circular gears for potted-seedling transplanter. *Transactions of the CSAE*, 2013; 29(8): 18–26. (in Chinese)
- [11] Ye B L, Li L, Yu G H, Liu A, Zhao Y. Dynamics analysis and test of rotary pick-up mechanism for vegetable pot-seedling. *Transactions of the CSAM*, 2014; 45(6): 70–78. (in Chinese)
- [12] Zhou M F, Xu J J, Tong J H, Yu G H, Zhao X, Xie J. Design and experiment of integrated automatic transplanting mechanism for taking and planting of flower plug seedlings. *Transactions of the CSAE*, 2018; 34(20): 44–51. (in Chinese)
- [13] Yin D Q, Wang J Z, Zhang S, Zhang N Y, Zhou M L. Optimized design and experiments of a rotary-extensive-type flowerpot seedling transplanting mechanism. *Int J Agric & Biol Eng*, 2019; 12(6): 45–50.
- [14] Zhao Y, Fan F L, Song Z C, Na M J, Zuo Y J, Feng Y, et al. Design and simulation of inverted vegetable pot seedling transplanting mechanism with conjugate cam. *Transactions of the CSAE*, 2014; 30(14): 8–16. (in Chinese)
- [15] Zhao X, Cui H, Dai L, Chen J, Ye B L. Kinematic analysis and experimental research on the seedling pick-up mechanism of a second-order free non-circular planetary gear system. *Appl Eng Agric*, 2017; 33(2): 169–179.
- [16] Sun L, Zhou Y Z, Chen X, Wu C Y, Zhang G F. Type synthesis and application of gear linkage transplanting mechanisms based on graph theory. *Trans ASABE*, 2019; 62(2): 515–528.
- [17] Han J, Qian W. On the solution of region-based planar four-bar motion generation. *Mech Mach Theory*, 2009; 44(2): 457–465.
- [18] Yang T, Han J Y, Yin L R. A unified synthesis method based on solution regions for four finitely separated and mixed “point-order” positions. *Mech Mach Theory*, 2011; 46(11): 1719–1731.
- [19] Ge Q J, Zhao Ping, Anurag P. Decomposition of planar burmester problems using kinematic mapping. In: *Decomposition of Planar Burmester Problems Using Kinematic Mapping*, Springer Science and Business Media B. V., 2013; pp.145–157.
- [20] Ge Q J, Zhao P, Purwar A, Li X Y. A novel approach to algebraic fitting of a pencil of quadrics for planar 4R motion synthesis. *J Comput Inf Sci Eng*, 2012; 12(4): 041003.
- [21] Zhao P, Ge X, Zi B, Ge Q J. Planar linkage synthesis for mixed exact and approximated motion realization via kinematic mapping. *Journal of Mechanisms and Robotics*, 2016; 8(5): 51004–51004.
- [22] Zhao P, Li X Y, Zhu L H, Zi B, Gee Q J. A novel motion synthesis approach with expandable solution space for planar linkages based on kinematic-mapping. *Mech Mach Theory*, 2016; 105: 164–175.
- [23] Sun L, Xu Y D, Huang H M, Wang Z F, Zhang G F, Wu C Y. Solution and Analysis of Transplanting Mechanism with Planetary Gear Train Based on Convexity of Pitch Curve. *Transactions of the CSAM*, 2018; 49(12): 83–92.
- [24] Han J Y, Yang T. On the solution of region-based planar six-bar motion generation for four finitely separated position. *ASME 2012 International Design Engineering Technical Conferences and Computers and Information in Engineering Conference American Society of Mechanical Engineers Digital Collection*, 2012; 441–449.
- [25] Han J, Li D Z, Gao T, Xia L, editors. Design method of non-circular geared five-bar linkage for passing pre-designated position points. 14th International Federation for the Promotion of Mechanism and Machine Science World Congress, IFToMM 2015, Taipei, October 25, 2015.
- [26] Qian W X, Han J Y. Synthesis Method for Planar Four-Bar Linkages Given Angle Displacements of Rotating Links. *Transactions of the Chinese Society of Agricultural Machinery*, 2009; 40(5): 222–226.